Available online at www.sciencedirect.com
ScienceDirect
Journal of the European Ceramic Society 27 (2007) 2423–2431
www.elsevier.com/locate/jeurceramsoc

Structural characterization of Na_2O–CaO–SiO_2 glass ceramics reinforced with electric arc furnace dust

I. Tsilika, Ph. Komninou *

Physics Department, Aristotle University of Thessaloniki, GR-54124 Thessaloniki, Greece

Received 9 April 2006; received in revised form 28 August 2006; accepted 10 September 2006
Available online 1 November 2006

Abstract

The microstructure of three different compositions of electric arc furnace dust (EAFD) from steel scrap recycling facilities mixed with cheap raw materials (SiO_2, Na_2O, CaO), treated under the same conditions were examined by means of X-ray diffraction (XRD), scanning electron microscopy (SEM) and transmission electron microscopy (TEM). Wollastonite-type crystals were identified as the major crystalline phases. The initial composition of the mixtures was found to influence the type of crystals formed. The distribution of the elements in the glass matrix and the crystals in the as-casted and crystallized samples as well as the role of EAFD in the crystallization process were studied in an attempt to understand the mechanism of wollastonite-type crystals formation.

Keywords: Electron microscopy; Glass ceramics; Electric arc furnace dust; Microstructure-final; Waste material

1. Introduction

Electric arc furnace dust (EAFD) is a solid waste produced during process of steel in steel scrap recycling facilities. It consists mainly of the contaminants of steel and its main components are zinc oxides (ZnO), lead oxide (PbO), and zinc ferrite ($ZnFe_2O_4$). Manganese oxide (MnO) and magnesium oxide (MgO), are contained in smaller amounts as well. The huge amount of annual production of EAFD (15,000 t/year) in Greece, along with its toxicity have raised the issue of developing environmental safe and low cost methods for the management of these solid wastes.

A continuously developing method of solid waste management is vitrification with the addition of batch materials.[1] Through vitrification, reduction of the volume of waste, destruction of the organic components and stabilization of the toxic ingredients are accomplished at the same time. The products of vitrification can, with further thermal treatment (nucleation and crystallization), be converted into glass ceramics with interesting mechanical, thermal and chemical properties.[2] The properties of the resulting glass ceramics are tailored by the initial composition of the glass and the heat treatment procedure.

In an attempt to solve the problem of management of EAFD wastes, Kavouras et al.[3] vitrified EAFD with cheap raw materials, namely $CaCO_3$, Na_2CO_3 and SiO_2 powders, at ambient pressure. The vitreous products were converted into glass ceramics by a two-stage heat treatment (nucleation and crystallization). Wollastonite ($CaSiO_3$) appeared to be the dominant crystalline phase. Depending on the initial composition, the resulting materials have been proved[3] to reveal different properties concerning their state of crystallization, morphology of the formed crystals and microhardness.

The main target of this work is to investigate, from the structural point of view, the inmobilization of EAFD and the possibility of utilizing the resulting glass ceramics into useful applications. Wollastonite, which has been found to dominate in the samples, is an important substance in ceramic and cement industries. It has traditionally been used as raw material for tiles, white paint, as a filler for resins or paper, as high frequency insulator and as machinable ceramic.[4] Thus, a thorough examination of the crystalline phases formed and the distribution of the elements of EAFD in the samples is performed during the whole process of the heat treatment (casting, nucleation, and crystallization) in order to understand the differences in the behavior of the devitrified materials and the mechanism that favors the for-

* Corresponding author. Tel.: +30 2310 998195; fax: +30 2310 998589.
E-mail address: komnhnoy@auth.gr (Ph. Komninou).

0955-2219/$ – see front matter © 2006 Elsevier Ltd. All rights reserved.
doi:10.1016/j.jeurceramsoc.2006.09.011

mation of the certain crystalline phases. In addition, the role of the elements of EAFD in the crystallization process is examined.

2. Experimental procedure

EAFD powder was mixed with SiO_2, Na_2CO_3, and $CaCO_3$ powders in various proportions. The wt% compositions of EAFD and of the resulting mixtures, named as EAFD 1, EAFD 2, EAFD 3, are shown in Tables 1 and 2, respectively. The solid mixtures were placed in a Pt crucible and they were heated in an electric furnace at ambient atmosphere at 1400 °C for 2 h. The resulting melts were poured on a stainless steel plate and were rapidly cooled down at room temperature. When cooled they were subjected to a two-stage isothermal treatment process at temperatures determined from DTA scans. Specifically, the samples were heated up to 680 °C for 15 min where nucleation initiated and then heated up to 900 °C for 30 min for their crystallization and crystal growth.

The resulting materials were characterized by X-ray diffraction analysis (XRD) using a Seifert 3003 powder diffractometer and Cu K_a1 radiation. Microstructure characterization was performed using electron microscopy techniques (EM). Scanning electron microscopy (SEM) observations and stoichiometric analysis of the materials were conducted in a JEOL JSM-840A microscope operated at 20 kV, equipped with an Oxford ISIS-300 energy dispersive spectrometry (EDS) analyzer. Specimens for transmission electron microscopy (TEM) and high-resolution TEM (HRTEM) investigations were initially thinned by mechanical grinding followed by ion-milling to reach electron transparency. TEM and HRTEM observations were carried out in a Jeol-2011 (point-to point resolution 0.19 nm and Cs = 0.5 mm) and a FEG STEM JEOL-2011 electron microscopes, both operated at 200 kV, the latter equipped with a Link EDS microprobe analyzer capable of analyzing particles of a few nanometers size. The microprobe analysis was employed complementary to the EDS analysis by SEM, where higher local resolution was demanded.

Table 1
Composition (wt%) of electric arc furnace dust (EAFD)

	EAFD
MgO (%)	0.8
Al_2O_3 (%)	1
SiO_2 (%)	4.5
K_2O (%)	1.5
CaO (%)	5.1
MnO (%)	3.7
Fe_2O_3 (%)	37.7
ZnO (%)	38.8
PbO (%)	6.9

Table 2
Compositions (wt%) of the resulting mixtures (EAFD 1, EAFD 2, EAFD 3)

	SiO_2 (%)	Na_2O (%)	CaO (%)	EAFD (%)
EAFD 1	55	10	15	20
EAFD 2	55	5	20	20
EAFD 3	55	5	25	15

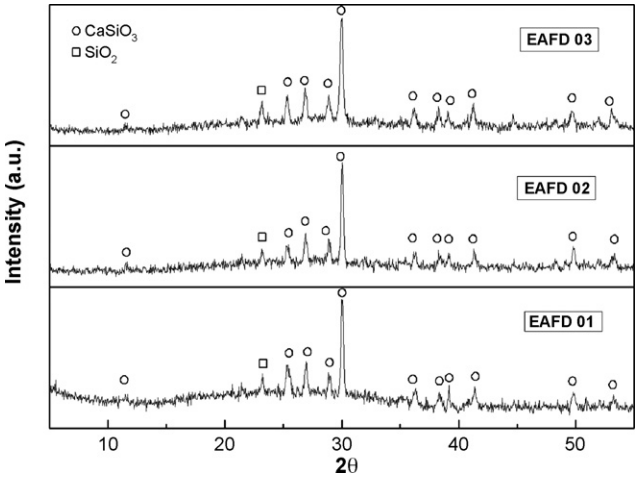

Fig. 1. X-ray diffractograms of EAFD 1, 2, 3.

3. Results

XRD measurements, presented in Fig. 1, showed that in all samples, despite their compositional differences, wollastonite is the dominant crystalline phase. A small peak of SiO_2 (tridymite) is also observed. The amorphous background present in the diffractograms (especially in EAFD 1) reveals that the materials are not fully crystallized.

TEM analysis was performed at both types of heat-treated materials: those presenting crystal nucleation and the crystallized ones. The former samples of all three compositions were found to be mainly amorphous, as can be seen in the electron diffraction pattern (EDP) of EAFD 3, illustrated in Fig. 2. The diffused rings together with the diffraction spots indicate early stages of crystallization. The crystallized samples revealed var-

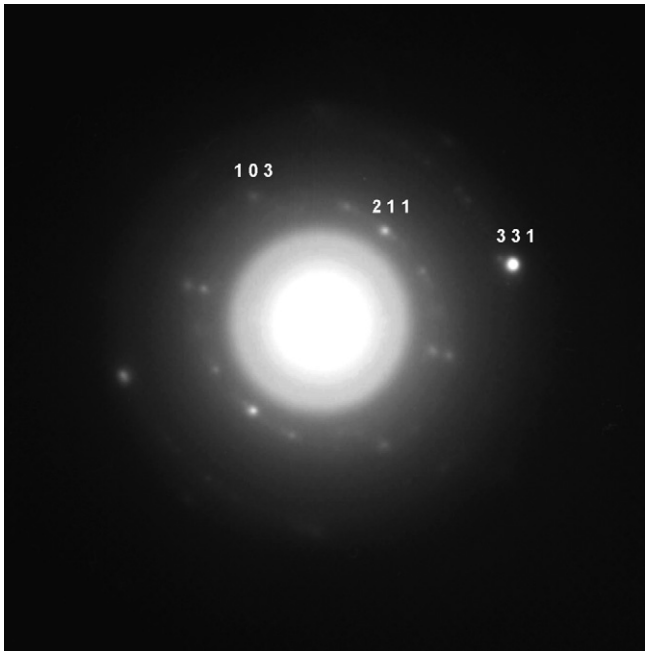

Fig. 2. EDP of the nucleated sample EAFD 3, showing early stages of crystallization of triclinic wollastonite.

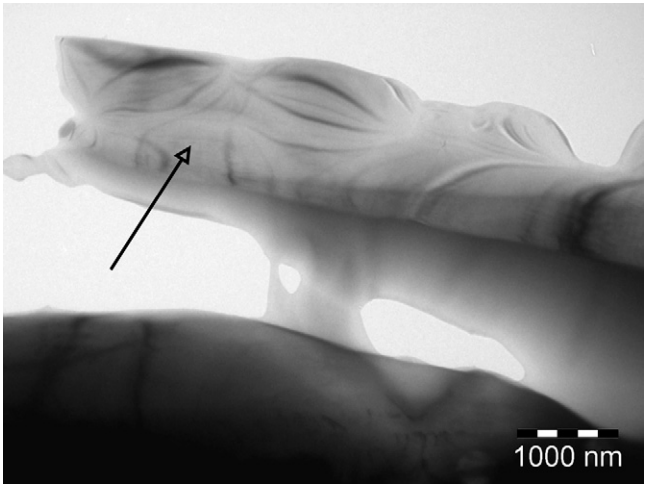

Fig. 3. Bright Field (BF) image of a wollastonite crystal formed inside the glass matrix.

ious types of crystal structures. Specifically the analysis of their EDPs showed wollastonite as the main crystal component and the existence of SiO_2 crystals in small amount, in accordance with XRD results. A Bright Field (BF) image of a needle like wollastonite crystal, formed inside the glass matrix of EAFD1 is shown in Fig. 3. Representative EDPs of the two crystal structures are shown in Fig. 4a and b. Fig. 4a depicts the [2 1 $\bar{2}$] zone axis of wollastonite taken from the sample EAFD 1, while Fig. 4b shows the [3 1 0] zone axis of SiO_2, taken from the same sample. Especially in EAFD 1, where the concentration of Na_2O is larger, the formation of (Na_2O, 3CaO, 6SiO_2) phase was also favored, as can been seen in the EDP of Fig. 4c, where the [0 1 2] zone axis of the specific phase was identified. The particular crystal structure was not detected by XRD probably due to its small amount present in the sample. Another structure was also identified by TEM at both EAFD 1, 2 with a space group and lattice parameters close to that of wollastonite. The EDP (Fig. 4d) of such a structure, belonging to EAFD 2, shows close resemblance to the EDP of the [1 $\bar{1}$ 0] zone axis of wollastonite.

In order to examine the homogeneity of the as-casted samples and the mechanism of crystallization, the elemental distribution is measured throughout the sample before the crystallization process. For this reason the EDS analyzer of SEM was used, the large diameter of the beam of which offers a better statistical analysis. The results of the EDS analysis of the samples EAFD 1, 2, 3 are presented in Fig. 5. From the EAFD elements only the distribution of Fe and Zn is depicted in the figure. This is because the particular elements exist in the sample in relatively large amounts, thus an accurate measurement could be

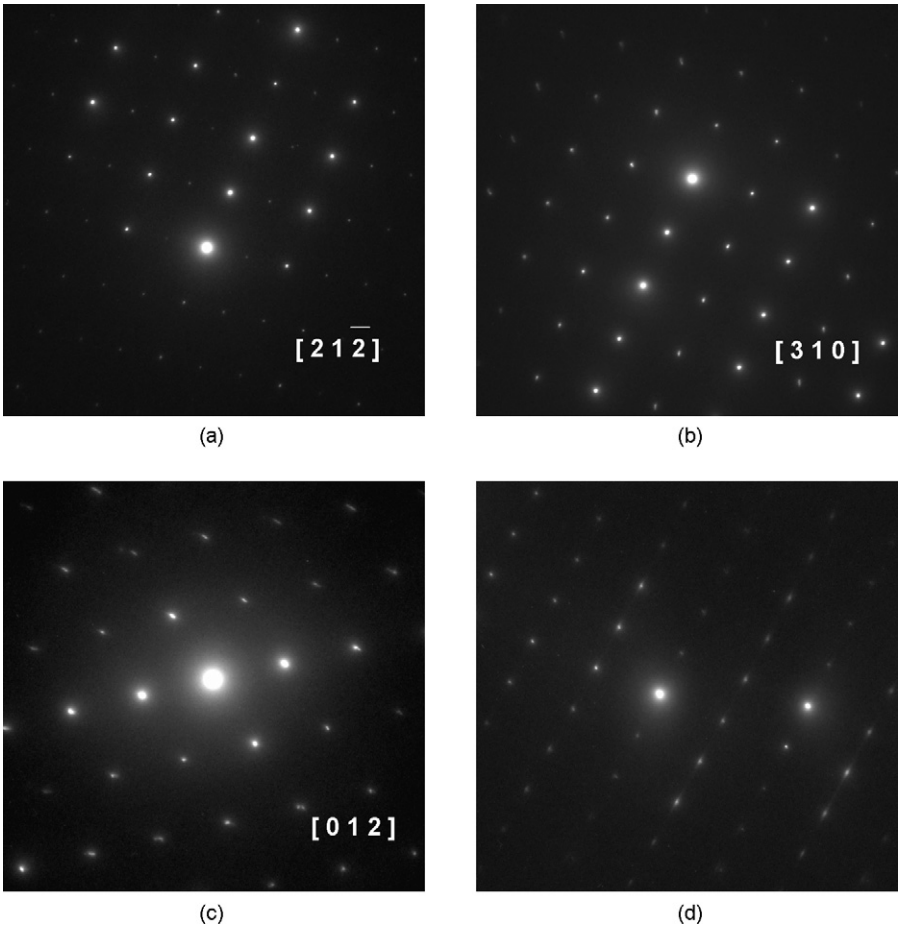

Fig. 4. EDP of: (a) the [21-2] zone axis of wollastonite, taken from the EAFD 1 sample, (b) the [3 1 0] zone axis of SiO_2, taken from the EAFD 1 sample, (c) [0 1 2] the zone axis of $Na_2Ca_3Si_6O_{16}$, taken from the EAFD 1 sample, (d) a crystal structure similar to wollastonite, taken from the EAFD 2 sample.

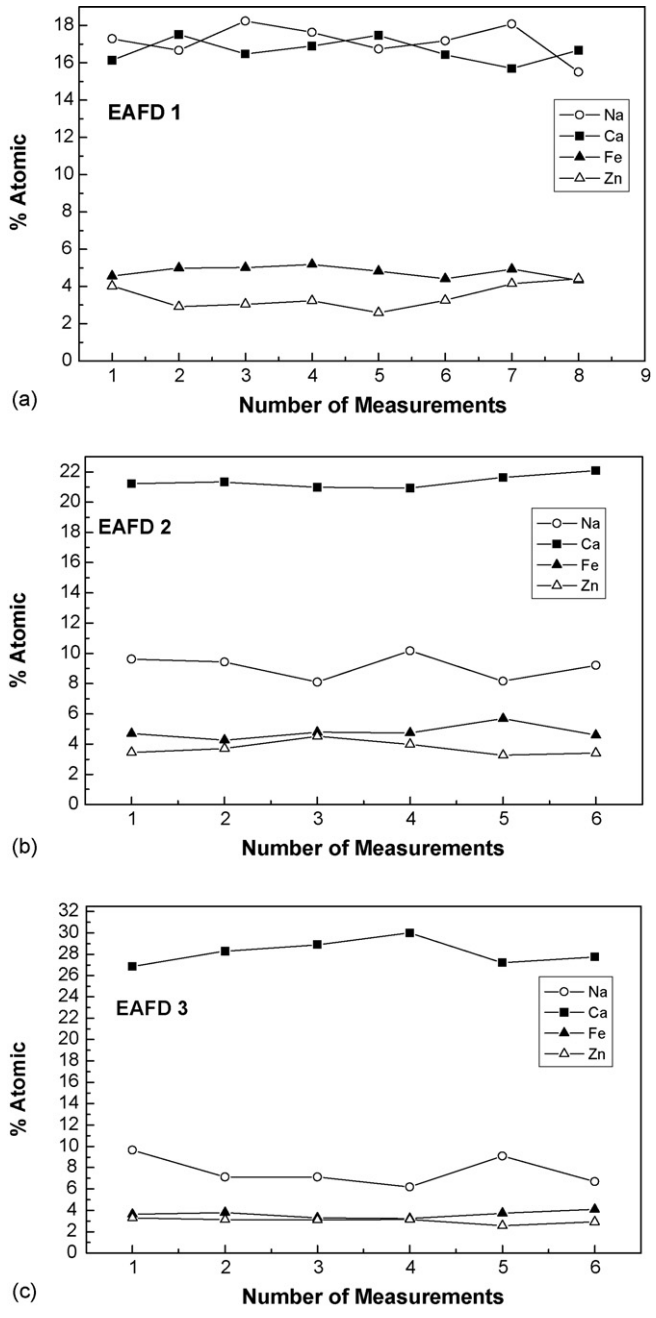

Fig. 5. Atomic percent of Ca, Na, Fe, Zn in the as-casted: (a) EAFD 1, (b) EAFD 2 and (c) EAFD 3 samples.

obtained. As it is made apparent, Na, Ca, Fe, Zn are dispersed almost homogeneously. It is obvious that the amount of atomic percent of the elements in the samples is dependent on their initial composition. Namely EAFD 3 that contains a larger amount of CaO relative to EAFD 1, 2, exhibits a higher average atomic percent in Ca.

After the crystallization procedure, crystals and glass matrix coexist in the samples. In order to examine the local variations of the compositions brought by the crystallization process, nanoprobe EDS analysis was taken from nanocrystals in the HRTEM observational mode. The small diameter of the probe size used ($1.2\,nm^{-1}$), allowed the stoichiometric analysis of the samples at the nanoscopic level.

The comparison of the residual glass matrix stoichiometry before and after the devitrification process shows differences in the concentration of Ca and the distribution of EAFD elements. In fact, as it is made apparent in the EDS spectra of Fig. 6, the calcium content is larger in the as-casted than in the glass matrix of crystallized EAFD 1, 2, 3, where the concentration of Ca is fairly small. In addition, the elements of EAFD are not homogeneously dispersed throughout the glass matrix of the crystallized samples, as was observed in the as-casted samples (Fig. 5). In the amorphous regions close to the crystals (Fig. 7a) EAFD concentration appears to be larger compared to the rest of the glass matrix (Fig. 7b).

As far as the crystalline areas of EAFD 1, 2 are concerned, differences in the calcium and EAFD content of the various crystals are also observed. Representative EDPs and their corresponding EDS spectra are shown in Fig. 8. Specifically there are crystals, with the symmetry of SiO_2 (Fig. 8a, EDP of [3 1 0] zone axis of SiO_2) in which the main component is Si, with small amounts of Ca, Na (Fig. 8b). In other crystals Si and Ca appear in higher percentage, while Na, Mn, Zn and Fe exist only as traces (Fig. 8d). These crystals show a wollastonite-type of structure, with small deviations in their d-spacings, namely in their lattice constants (Fig. 8c). A third type involves crystals which contain Si, Ca, Na, Fe, and Mn in such amount that (Ca, Na, Fe, Mn)/Si = 1/1 (Fig. 8f). The particular crystals have

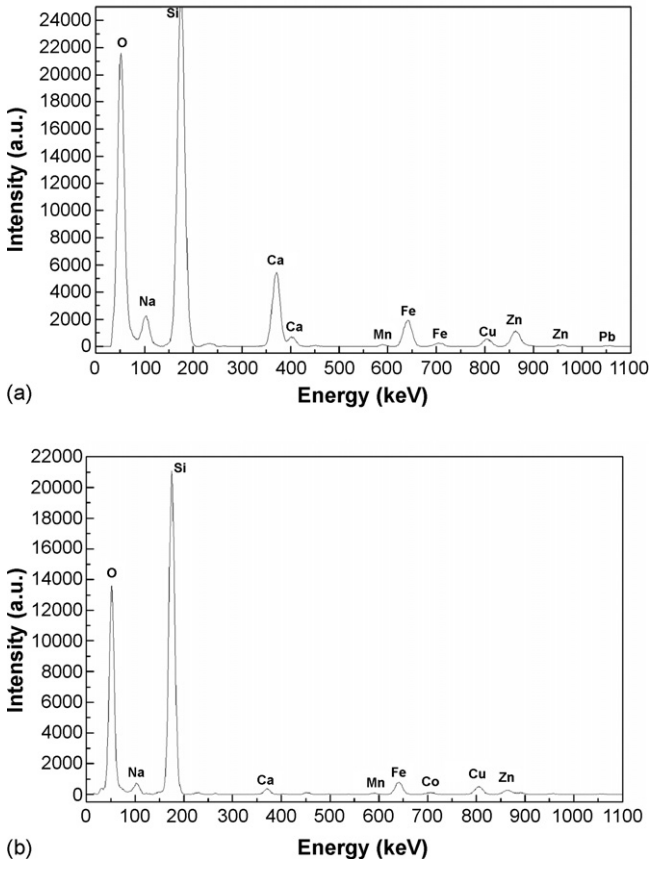

Fig. 6. Representative EDS analysis taken from nanocrystals of EAFD 1 in the HRTEM observational mode: (a) in the as-casted sample, (b) in the glass matrix of the crystallized sample.

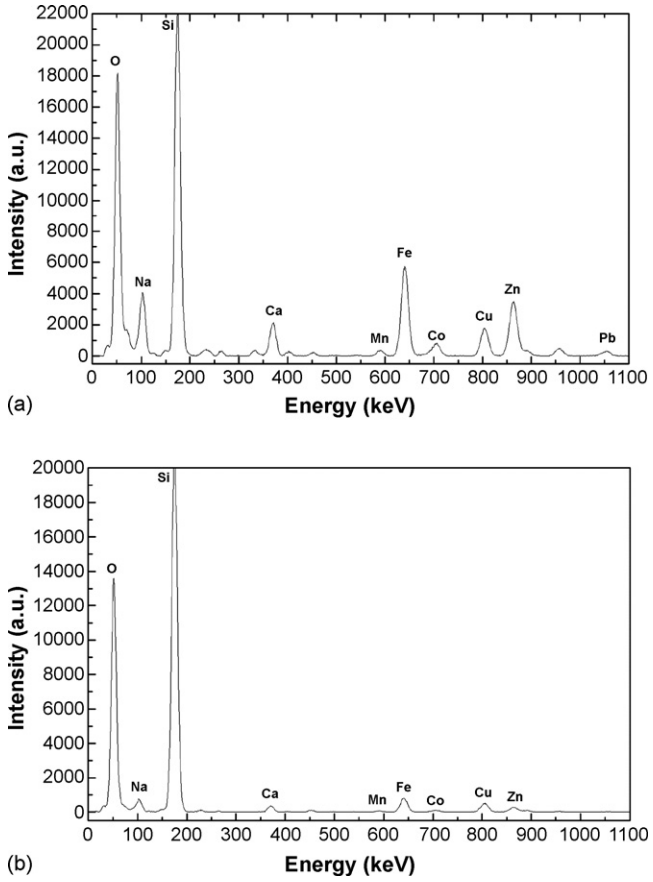

Fig. 7. Representative EDS analysis taken from nanocrystals of the crystallized EAFD 1 in the HRTEM observational mode: (a) in the glass matrix close to a crystal, (b) in the rest of the glass matrix.

the wollastonite structure (Fig. 8e, EDP of [21-2] zone axis of wollastonite).

When the calcium content is further increased (EAFD 3) at the expense of EAFD, the crystals formed, have Ca, Si as main components. EAFD appears in the crystals mainly as traces and less often in small amounts. The Ca/Si ratio fluctuates between 0.8 and 0.9 in most crystals. This is obvious in Fig. 9, where the EDP of the [0 0 1] zone axis of wollastonite along with the corresponding EDS spectrum is depicted. The stoichiometry of the formed $CaSiO_3$ crystals approaches the ideal one (Ca/Si = 1/1).

4. Discussion

The crystal phases stable at the composition of the samples are depicted in the phase diagram shown in Fig. 10.[5] It is apparent that the composition of EAFD 1 (denoted by 1 in the phase diagram) corresponds to the crystalline phase $Na_2Ca_3Si_6O_{16}$. However, the particular phase is stable at higher temperatures, namely higher energies compared to the conditions of crystallization of EAFD 1. In the sample (EAFD 1) examined, the majority of the crystals are found to belong to the wollastonite structure. Only small areas of the sample were identified as $Na_2Ca_3Si_6O_{16}$. As the concentration of calcium increases at the expense of sodium (EAFD 2, 3), the concentration of the mixture is moved to points 2 and 3 in the phase diagram (Fig. 10).[5]

In the crystal structures formed in all the samples, an important role plays the presence of EAFD which has not been taken into account in the phase diagram. As it has been mentioned, EAFD consists of a mixture of various oxides. According to Alizadeh et al.,[6] the presence of certain oxides (Fe_2O_3, Cr_2O_3, V_2O_5, etc.) or combinations of them, act as nucleating agents who have been proved not only to promote bulk crystallization but also to influence the nature and the amount of phases crystallized, namely different phases crystallize at the presence of different nucleating agents.

A clear proof of this assumption is shown in Table 3. In the sample EAFD 1 wollastonite appears as the dominant phase and $Na_2Ca_3Si_6O_{16}$ as a minor phase. Previous experiments[7] performed on samples with similar parent glass composition as EAFD 1, (sample 1: all EAFD is substituted by CaO), have indicated the presence of $Na_2Ca_3Si_6O_{16}$ as the dominant crystalline phase and wollastonite as a minor phase, indicating that EAFD act as a nucleating agent which promotes wollastonite formation.

In addition, the crystallization of wollastonite in our samples at relatively low temperature (900 °C), compared with the one indicated in the phase diagram (1100 °C), also may be attributed to the presence of the oxides of EAFD. Rizkalla et al.[8] have reported that the presence of P_2O_5 in the parent glass (SiO_2, CaO, and Na_2O) lowers the activation energy of crystallization of wollastonite. Consequently, the elements of EAFD, especially Fe, Zn seem to play an important role in the crystallization mechanism.

According to Rincon et al.[9] during bulk crystallization, Fe ions show tendency to diffuse to the surface. Supposing that each wollastonite crystal acts as a small bulk crystal, it may be assumed that the presence of Fe, Zn in our samples initially facilitate crystallization, while during crystallization diffuse to the glass matrix and are distributed around crystals.[10] This theory is in accordance with the EDS analysis taken from nanocrystals of EAFD 1, 2, 3 in the HRTEM observational mode. The specific analysis showed that the concentration of EAFD in the amor-

Table 3
Crystalline phases at different compositions

Sample name	Chemical composition (wt%)				Crystalline phases
	SiO_2	CaO	Na_2O	EAFD	
Sample 1[5]	55	34	11	–	Major phase: $Na_2Ca_3Si_6O_{16}$ Minor phases: wollastonite, $Na_2Ca_2Si_3O_9$, Na_2CaSiO_4
EAFD 1	55	15	10	20	Major phase: wollastonite Minor phases: $Na_2Ca_3Si_6O_{16}$, SiO_2

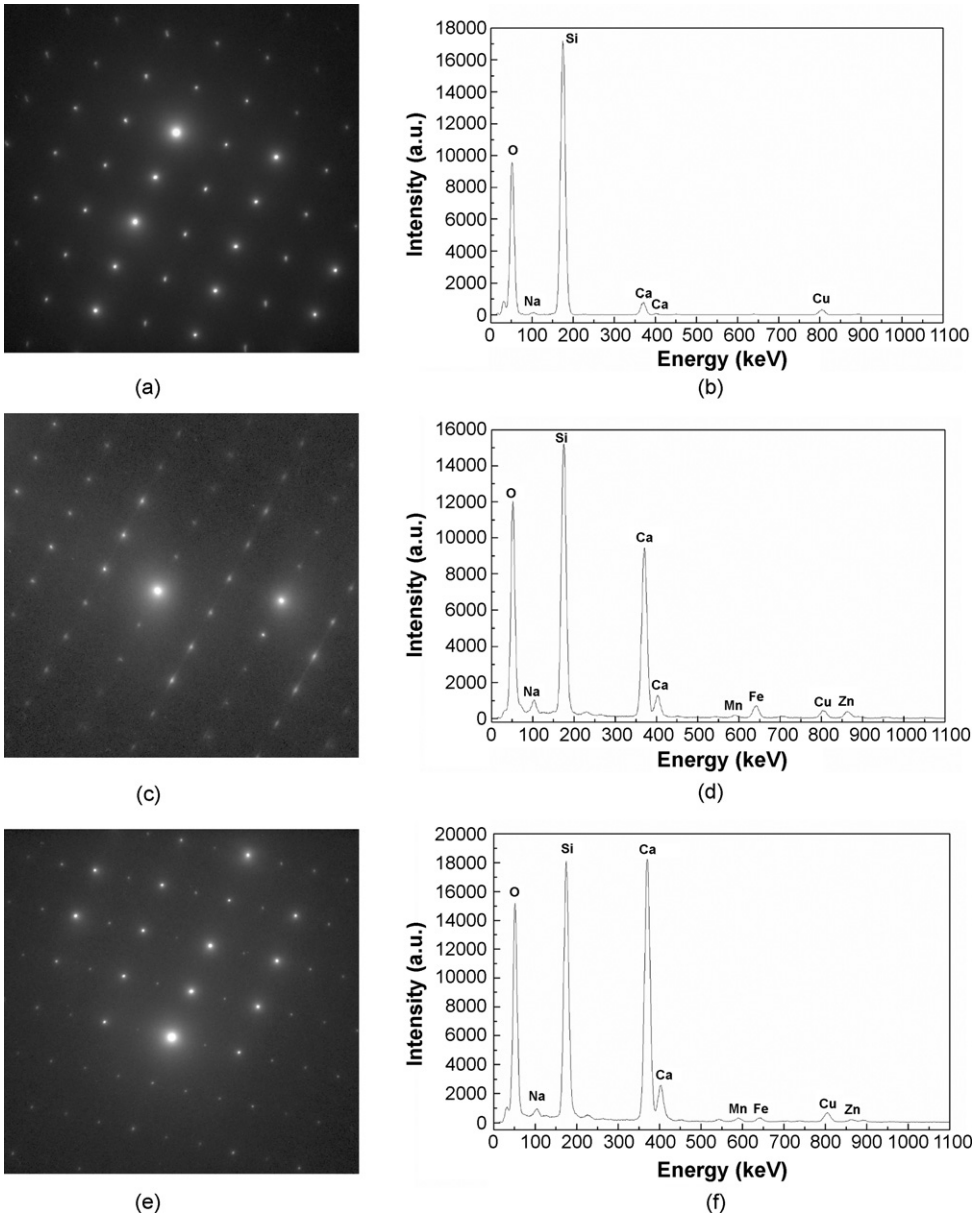

Fig. 8. (a) EDP of a crystal of EAFD 1 with the SiO_2 structure, (b) the corresponding EDS analysis, with Si as the main component, (c) EDP of a crystal of EAFD 2 with a wollastonite-type structure, (d) the corresponding EDS analysis, with Si, Ca, Na, as main components and traces of EAFD, (e) EDP of a crystal of EAFD 1 with the wollastonite structure, (f) the corresponding EDS analysis, with (Ca, Na, Fe, Mn)/Si:1/1.

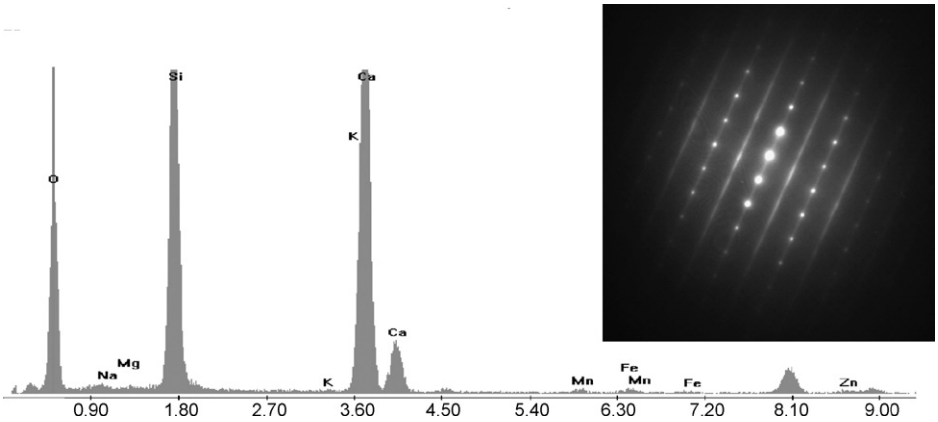

Fig. 9. EDP of the [1 0 0] zone axis of a wollastonite crystal of EAFD 3 with Ca/Si ∼ 1 and the corresponding EDS analysis.

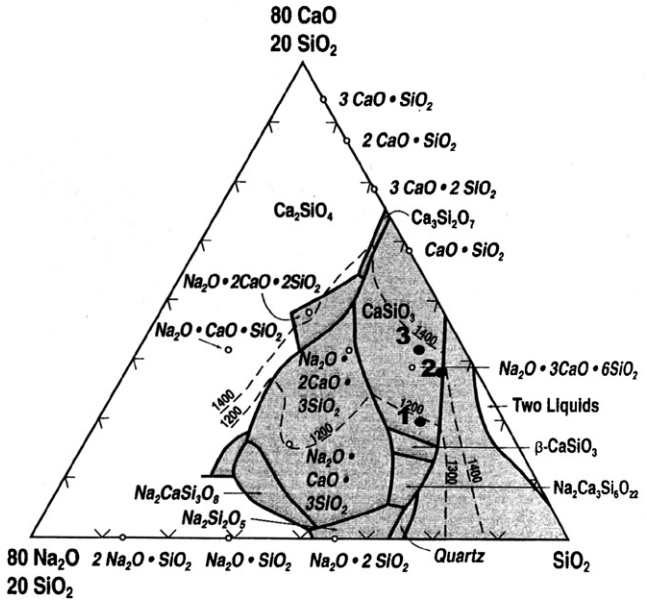

Fig. 10. Phase diagram of $CaO–Na_2O–SiO_2$ system.[5]

phous areas, surrounding the crystallized areas of wollastonite, is large and small or zero inside the crystals. Such a HRTEM image (taken from the EAFD 1 sample) and the corresponding EDS spectra are presented in Fig. 11.

The role of EAFD as a nucleating agent may explain also the reason why the particular elements are not homogeneously dispersed in the glass matrix of the crystallized samples. As it has been discussed, during crystallization EAFD promotes crystallization of wollastonite and diffuses to the surrounding glass matrix. As a result the elements of EAFD, after the crystallization process are not homogeneously dispersed in all the material, being in small amount or absent in the crystallized areas (Fig. 11), showing local maxima in the amorphous regions near the crystals (Figs. 11 and 7a) and being almost absent in the rest of the glass matrix (Fig. 7b).

The crystallization of wollastonite requires a considerable amount of Ca. That is why the glass matrix of the devitrified samples has a smaller amount of Ca. Namely calcium is gathered in the regions to be crystallized in order to form $CaSiO_3$. As a result the neighboring regions are depleted from calcium.

It has been mentioned that wollastonite ($CaSiO_3$) is the crystalline phase that is favored under certain conditions. The stoichiometry of $CaSiO_3$ requires Ca/Si:1/1. In the samples examined the amount of calcium is not adequate to meet this requirement. Consequently crystals from which the EDP of Fig. 8c and the EDS spectrum of Fig. 8d were taken, are formed with deviations in lattice parameters and stoichiometry of the ideal wollastonite structure.

It is reasonable to assume that the type of crystals formed depend on the local fluctuations of the chemical environment. So the crystals with Si in large amount, Ca in smaller amount and traces of Na, Mn, Zn, and Fe (Fig. 8c) are expected to be found in regions where the nucleating agents of EAFD are present. These crystals are attributed to wollastonite-type crystals, because this structure is identified by the EDP (Fig. 8c) and favored under the conditions, even though Ca/Si < 1/1. Small amount of EAFD elements occupy the Ca sites in the $CaSiO_3$ structure and form (Ca, Na, Fe, Mn, Zn)SiO_3 crystals. When Ca/Si is sufficiently large (Fig. 8f) (Ca, Na, Fe, Mn, Zn)/Si:1/1 crystals are also observed (the third type of crystals, Fig. 8e).

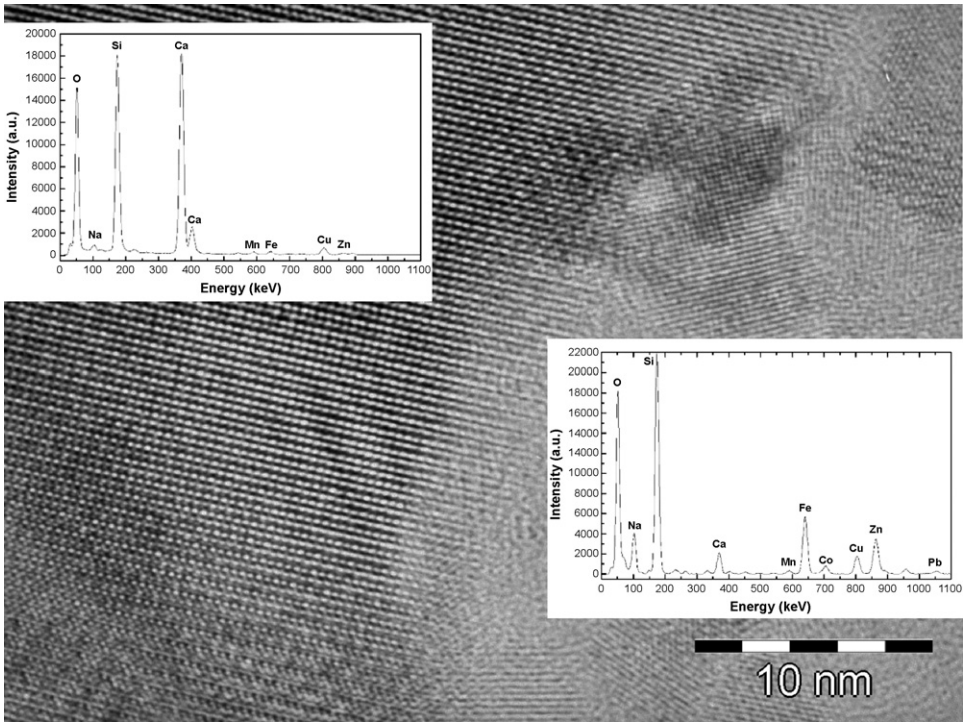

Fig. 11. HRTEM image of a crystallized ([1 0 0] zone axis) and an amorphous region and their corresponding EDS nanoanalysis.

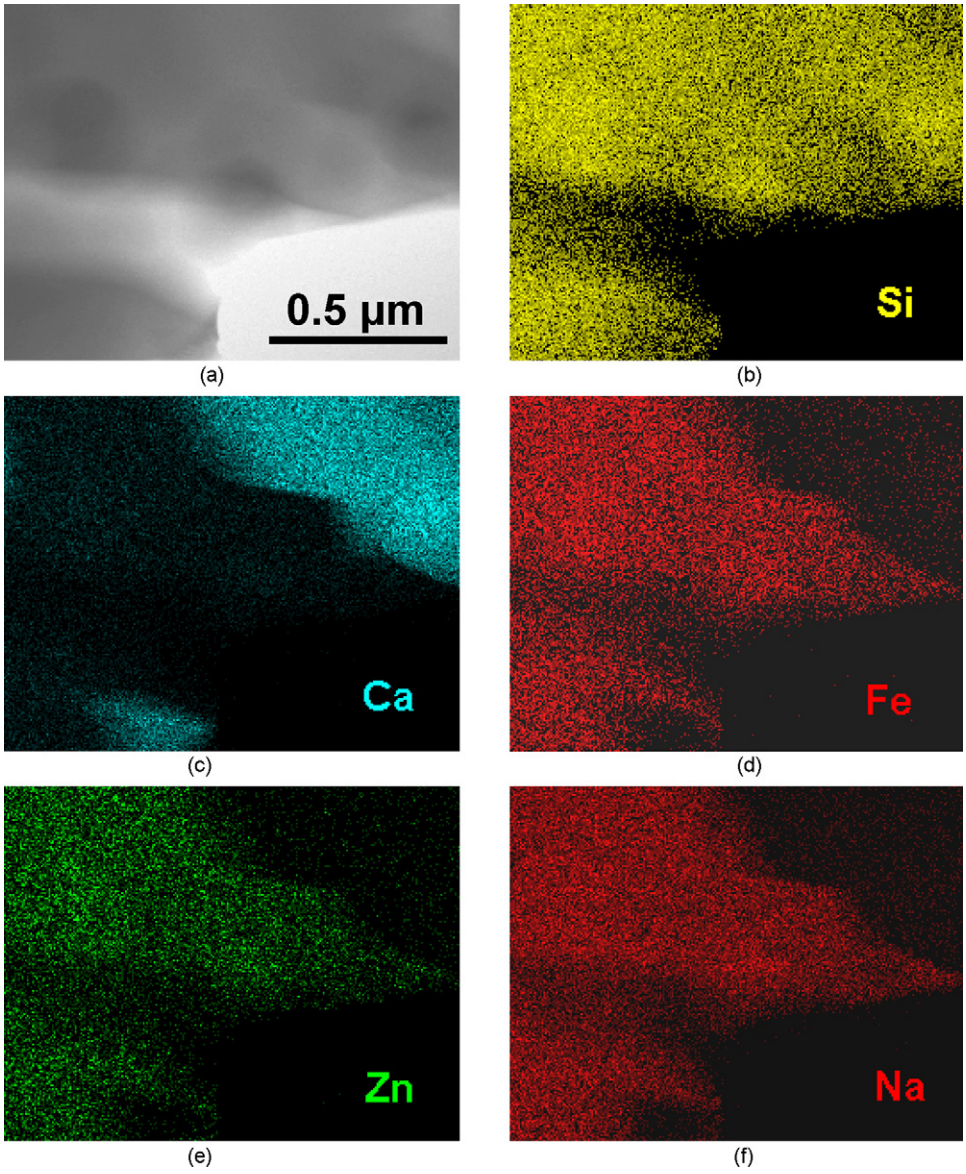

Fig. 12. The distribution of the elements Ca, Si, Fe, Zn, Na in an area containing crystals and glass matrix (X-ray mapping). (a) STEM image, (b) Si content, (c) Ca content, (d) Fe content, (e) Zn content, (f) Na content.

The crystals with the structure of SiO_2 (Fig. 8a) and with main component Si and small amount of Ca, Na (Fig. 8b) are expected to appear in areas of the sample with small calcium and EAFD content and especially in EAFD 1 where the concentration of Ca is smaller. The particular crystals may be attributed to SiO_2 glass residuals, which were also identified in XRD measurements.

When calcium content is further increased (EAFD 3) the Ca/Si ratio is more close to unity. As a result more crystals with the $CaSiO_3$ stoichiometry and the structure of wollastonite are formed. The amount of crystals with Ca/Si < 1 is significantly decreased, the elements of EAFD disperse into the glass matrix and a better crystallization and stabilization of the waste is accomplished. So the addition of calcium has resulted in the formation of crystallized samples with the stoichiometry and structure of wollastonite, while EAFD elements are not incorporated any more in the crystal structure, showing tendency to diffuse to the chemical inert matrix where they are stabilized.

It is worth noticing the role of Zn^{++} in the wollastonite-type crystals. Zn is classified among the intermediate species, acting either as a glass network former occupying tetrahedral sites or as a modifier occupying octahedral sites.[11] In the present case, Zn^{++} as well as Fe^{++}, seems to substitute partially Ca^{++} in the structure of wollastonite, giving rise to a solid solution of (Ca, Zn, Fe)SiO_3 wollastonite structure.

As it was mentioned the majority of EAFD elements of the devitrified materials appear in the matrix surrounding the crystals (Fig. 7a). This is also evident from Fig. 12, where a well crystallized area of EAFD 3 is illustrated together with the X-ray maps of some of the EAFD elements. The crystals of wollastonite are depicted from their large concentration of Ca

(Fig. 12c). The particular areas are depleted from the EAFD elements (Fig. 12d, e and f). The Fe, Zn, Na elements are distributed in the matrix around the crystals. As it is expected silicon, as the glass network former, is homogeneously dispersed in all the samples. The transparent area in the middle of the picture (Fig. 12a) is due to the thickness variation of the sample.

5. Conclusions

The microstructure and the distribution of elements of vitrified industrial waste (electric arc furnace dust) from steel scrap recycling facilities were examined during the whole crystallization process. The local chemical environment seems to determine the different types of crystals formed. As the concentration of Ca increases in the initial composition, the Ca/Si ratio approaches unity and more crystals of the ideal wollastonite structure and stoichiometry are formed. The elements of EAFD seem to facilitate wollastonite formation and show tendency to diffuse to the chemical inert matrix near the crystals after crystallization, where they are stabilized.

Acknowledgements

The authors are grateful to P. Kavouras and G. Kaimakamis for the growth of specimens. They also wish to thank S. Kokkou, E. Pavlidou, Th. Karakostas, Th. Kehagias and G. Nouet for their valuable collaboration and fruitful discussions.

References

1. Conner, J. R. and Hoeffner, S. L., A critical review of stabilization/solidification technology. *Crit. Rev. Environ. Sci. Tech.*, 1998, **28**, 397–462.
2. Torres, F. J. and Alarcon, J., Pyroxene-based glass-ceramics as glazes for floor tiles. *J. Eur. Ceram. Soc.*, 2005, **25**, 349–355.
3. Kavouras, P., Kehagias, Th., Tsilika, I., Chrissafis, K., Kaimakamis, G., Papadopoulos, D., Kokkou, S., Komninou, Ph. and Karakostas, Th., Glass-ceramic materials from electric arc furnace dust. *J. Hazard. Mater.*, 2007, **139**, 424–429.
4. Yun, Y. H., Yun, S. D., Park, H. R., Lee, Y. K. and Youn, Y. N., Preparation of β-wollastonite glass ceramics. *J. Mater. Synth. Proces.*, 2002, **4**, 205–209.
5. Höland, W. and Beall, G., *Glass-Ceramic Technology*. The American Ceramic Society, Ohio, 2002, p. 136.
6. Alizadeh, P. and Marghussian, V. K., Effect of nucleating agents on the crystallization behavior and microstructure of SiO_2–CaO–MgO (Na_2O) glass ceramics. *J. Eur. Ceram. Soc.*, 2000, **20**, 775–782.
7. Tsilika, I., Kaimakamis G., Terzidis Ch., Kehagias Th., Komninou Ph. and Karakostas Th., Proceedings of the XX Greek Conference of Solid State Physics, 2007, in press.
8. Rizkalla, A. S., Jones, D. W., Clarke, D. B. and Hall, G. C., Crystallization of experimental bioactive glass compositions. *J. Biomed. Mat. Res.*, 1996, **32**, 119–124.
9. Rincon, J. Ma. and Callejas, P., Microanalysis of the surface in glass-ceramics obtained from muscovite amblygonite. *J. Mater. Sci.*, 1988, **23**, 1042–1049.
10. Romero, M., Rincon, J. Ma., Rawlings, R. D. and Boccaccini, A. R., Use of vitrified urban incinerator waste as raw material for production of sintered glass ceramics. *Mater. Res. Bull.*, 2001, **36**, 383–395.
11. Vogel, W., *Chemistry of Glass*. American Ceramic Society, Columbus, Ohio, 1985.